JOURNAL OF QUATERNARY SCIENCE (2015) **30**(8) 817–829 ISSN 0267-8179. DOI: 10.1002/jqs.2818

Pollen–climate reconstruction from northern South Island, New Zealand (41°S), reveals varying high- and low-latitude teleconnections over the last 16 000 years

IGNACIO A. JARA,[1]* REWI M. NEWNHAM,[1] MARCUS J. VANDERGOES,[2] COURTNEY R. FOSTER,[3] DAVID J. LOWE,[3] JANET M. WILMSHURST,[4,5] PATRICIO I. MORENO,[6] JAMES A. RENWICK[1] and ALINE M. HOMES[1]

[1]School of Geography Environment & Earth Sciences, Victoria University of Wellington, POBox 600, Wellington 6140, New Zealand

[2]GNS Science, Lower Hutt, New Zealand

[3]School of Science, University of Waikato, Hamilton, New Zealand

[4]Landcare Research, Lincoln, Canterbury, New Zealand

[5]School of Environment, University of Auckland, Auckland, New Zealand

[6]Department of Ecological Sciences and Millennium Institute of Ecology and Biogeography, Universidad de Chile, Las Palmeras, Santiago, Chile

Received 9 April 2015; Revised 9 October 2015; Accepted 21 October 2015

ABSTRACT: We present a 16 000-year vegetation and climate reconstruction from pollen and plant macrofossil records obtained at a small alpine lake in South Island, New Zealand (41°S). The expansion of lowland forest taxa suggests a lifting of the altitudinal forest limits because of a warming pulse between 13 and 10k cal a BP and between 7 and 6k cal a BP, while their decline relative to upland forest taxa indicates cooling phases between 10 and 7k cal a BP and over the last 3000 years. The modern treeline was first established locally by 9.7k cal a BP. Forest persisted at the site until 3k cal a BP then disappeared from the record. Close correspondence between the temperature trends inferred from the pollen and macrofossil records and proxies from Antarctica and the Southern Ocean suggests a strong teleconnection between New Zealand and the Southern Hemisphere high-latitudes between 15 and 6k cal a BP. We note that the breakdown of this coupling, a cooling trend in Adelaide Tarn and the local disappearance of beech forest after 3k cal a BP occur during a period of increased frequency of El Niño events, suggesting an enhanced teleconnection with the low-latitudes during the late Holocene.

KEYWORDS: El Niño Southern Oscillation; New Zealand; plant macrofossils; pollen; SAM; treeline.

Introduction

New Zealand is particularly well suited to climate reconstructions using vegetation archives because of the climate sensitivity of its vegetation and a late settlement history that precludes anthropogenic disturbance for all but the last 750 years (Newnham *et al.*, 1999; Wilmshurst *et al.*, 2008; Barrell *et al.*, 2013). Critically, its location straddling the southern mid-latitudes (34–47°S) makes it sensitive to atmospheric variability originating in both the tropical Pacific to the north and the extra-tropical Southern Ocean to the south (Kidson *et al.*, 2002; Ummenhofer and England, 2007). These teleconnections strongly influence the modern inter-annual climate variability observed in New Zealand, yet little is known about how they may have operated before the instrumental era. There is therefore a pressing need to develop well-dated sensitive climate proxies from New Zealand's natural archives that can reveal the influence of low- and high-latitude atmospheric circulation over New Zealand climate in a longer-term context.

Here we present a high-resolution pollen record spanning the last 16 000 years from a small lake, Adelaide Tarn, near the modern treeline in Northwest Nelson, a mountainous region in central New Zealand (41°S). Pollen data are complemented by plant macrofossil evidence to document the local and regional vegetation and climate history. A vegetation-based reconstruction from this sector is pertinent to large-scale climate teleconnections for two main reasons. First, Northwest Nelson is located on the current northern margin of year-round influence of the southern westerly wind belt, and therefore its vegetation history should reflect latitudinal shifts in this hemispheric-wide extra-tropical atmospheric circulation system. Second, Adelaide Tarn is situated at the present-day treeline in a region of strong relief, which permits the detection of climate-driven altitudinal shifts of this major ecological boundary and of other vegetation units downslope.

*Correspondence: I. A. Jara, as above
E-mail: ignacio.jaraparra@vuw.ac.nz

Study region

Physical setting

Northwest Nelson (40–41°S, 172–173°W), in the north-west corner of New Zealand's South Island, is a region of mostly high relief and rugged topography representing the northernmost part of the Southern Alps (Fig. 1). The highest peaks, ranging from 1600 to 1800 m in elevation, occur in the predominantly granitic Tasman Mountains. The region lacks modern glaciers, unlike higher elevations in the central and Southern Alps to the south, but there is unequivocal geomorphic evidence for alpine glaciation during the Pleistocene (Shulmeister *et al.*, 2005; McCarthy *et al.*, 2008).

Adelaide Tarn (40°56′S, 172°32′W; 1250 m) is a small lake (0.06 km^2) sitting in a glacial cirque (3.8 km^2) in the Douglas Range amid the Tasman Mountains. With a current maximum water depth of 7.6 m, Adelaide Tarn is fed by a single inlet on its south-eastern border and drained by a single outlet on its north-western edge (Fig. 1).

Atmospheric circulation

The position of New Zealand in the mid-latitudes of the southern Pacific Ocean and its topography marked by the

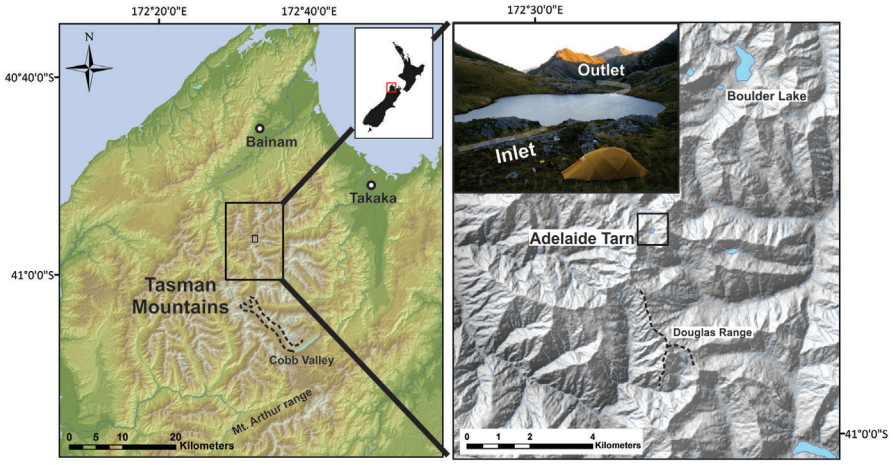

Figure 1. Digital elevation model of the Northwest Nelson region and the geomorphic emplacement of Adelaide Tarn. The left-hand image includes the climate stations and other physiographic units mentioned in the text. The superimposed photograph to the right shows Adelaide Tarn looking towards the north and highlights the lake's inlet and outlet. Photo courtesy of Marcus J. Vandergoes.

presence of axial cordilleras are the main factors determining its broad-scale climate regimes. A north–south gradient in mainland temperatures results from the interaction between warm sub-tropical Pacific and cold sub-Antarctic oceanic waters. The oceanic setting serves to moderate the pronounced seasonal fluctuations that characterize the climate of more continental landmasses at equivalent latitudes. The main pattern of precipitation regimes across the country follows the east–west gradient imposed by the intersection of the predominant westerly circulation with the topographical barrier of the axial cordilleras. This pattern results in relatively high precipitation totals in western regions (up to 10 000 mm a^{-1}) and much lower precipitation in the east (500 mm a^{-1}).

A significant amount of the modern climate variability across New Zealand is explained by low- and high-latitude modes of climate variability such as El Niño Southern Oscillation and the Southern Annular Mode (SAM) (Kidson *et al.*, 2002; Kidston *et al.*, 2009). In general, La Niña years are associated with stronger sub-tropical easterly flow which results in overall warmer conditions across the country and higher annual precipitation in the north and east, whereas El Niño years are associated with stronger extra-tropical south-westerly flow resulting in overall higher annual rainfall and lower temperatures in the southern and western districts (Kidson and Renwick, 2002; Thompson *et al.*, 2011; Figure 2). Positive phases of SAM are associated with a reduction of the westerly flow over New Zealand resulting in decreased precipitation over western districts and higher temperatures over most of the country, while the opposite scenario is observed during negative phases (Renwick and Thompson, 2006; Fig. 2).

Data from climate stations in Northwest Nelson derived from the National Climate Database (www.cliflo.niwa.co.nz) provide an adequate representation of the regional climate setting. High annual precipitation with minor seasonal differences prevails in the relatively flat and exposed northern areas as the westerly fronts are complemented by a substantial presence of storms from the north during summer months. The eastern part of Northwest Nelson, on the lee side of the Tasman Mountains, has a more continental climate with significantly lower annual precipitation because of a strong rain shadow effect, and a marked precipitation minimum during summer resulting from a meridional shift of the zone of maximum westerly sourced precipitation. Mean annual temperatures in Northwest Nelson vary from 12.5 °C at 25 m to 8.5 °C at 823 m. These values give a regional lapse rate of 5.5 °C per 1000 m, which is close to the environmental lapse rate calculated for the central Southern Alps (6.0 °C per 1000 m; Hales and Roering, 2005). Based on its elevation (1250 m), the regional lapse rate and its position relative to the closest climate stations, we estimate Adelaide Tarn to have mean annual temperatures of ~6.2 °C with total annual precipitation ≥2500 mm, resulting predominantly from the westerly circulation. However, its relatively northern location is likely to result in summer precipitation minima, similar to those of the eastern areas of Northwest Nelson.

Vegetation in Northwest Nelson

Native forest in Northwest Nelson can be broadly classified into two main forest communities: conifer–broadleaf forest at lower elevations and *Fuscospora/Lophozonia* (southern beech) forest at higher elevations up to the treeline (Wardle,

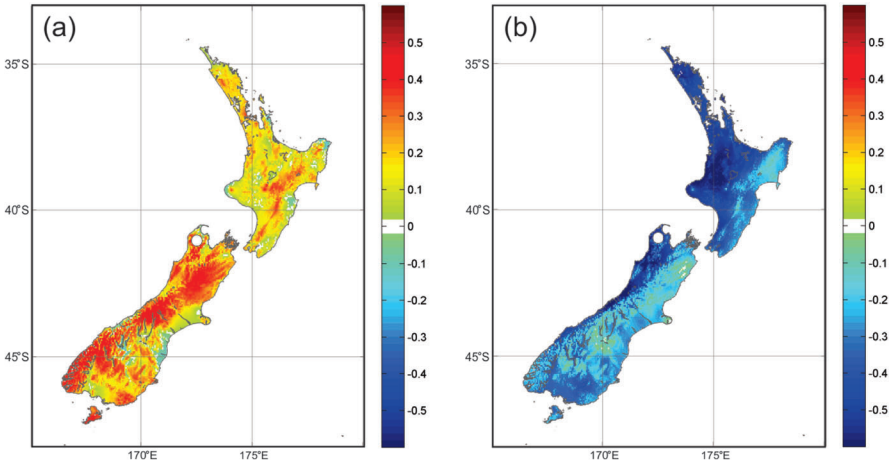

Figure 2. Correlation maps for mean annual (May–April) surface temperatures and (a) the SAM index, and (b) El Niño 3.4 sea surface temperature. Both correlations are calculated based on a 1979–2008 regression. The white circle denotes the location of Adelaide Tarn.

1991). The altitudinal distribution of these communities is primarily controlled by regional temperature, and thereafter by local environmental factors such as soil moisture and quality, aspect, and slope. Therefore, the altitudinal zonation of vegetation in Northwest Nelson can be used as a modern analogue for interpreting past changes in temperature from pollen profiles in the region.

Lowland to montane areas at elevations lower than 600 m, where soils are relatively fertile and temperatures moderate throughout the year, support a relatively diverse and structurally complex conifer–broadleaf forest community. The forest canopy is mainly dominated by the tall conifer *Dacrydium cupressinum* and may include others such as *Prumnopitys taxifolia*, *P. ferruginea*, *Podocarpus totara* and *Dacrycarpus dacrydiodies* in poorly drained sites. The sub-canopy typically comprises angiosperm trees including *Metrosideros robusta*, *M. umbrellata*, *Weinmannia racemosa* and *Coprosma lucida*, while the understorey features the tree-ferns *Cyathea smithii* and *Dicksonia squarrosa*, epiphytes such as *Griselinia lucida* and the fern *Asplenium polyodon*, lianas such as *M. fulgens* and *M. diffusa*, and several shrub and herb species including *Raukaua simplex* and *Myrsine australis*. In the mountainous regions above 600 m, where soils are generally less fertile and temperatures lower, conifer–broadleaf forest is usually replaced by the floristically less diverse southern beech forest. Notably, in certain areas in the Cobb Valley subalpine–conifer forest featuring *Phyllocladus alpinus* and *Halocarpus biformis* develops largely in the absence of southern beech species. Otherwise, *Lophozonia menziesii* or *Fuscospora cliffortioides* typically dominate the southern beech forest canopy with an understorey represented by an impoverished version of the conifer–broadleaf forest sub-canopy described above. The most common species occurring beneath the canopy are *Coprosma macrocarpa*, *Leucopogon fasciculatus*, *Leptecophylla juniperina*, *Kunzea ericoides*, and shrubs forms of *P. alpinus* and *H. biformis*.

The average regional treeline elevation is about 1350 m, 30–100 m above the elevation of Adelaide Tarn. However, because of the rugged regional topography the treeline may descend to 1200 m in steep bedrock gullies or steep slopes with thin soils (such as at Adelaide Tarn), or ascend to 1500 m in rocky well-drained slopes and ridges (Williams, 1993). In addition, goats, sheep and several other grazing animals introduced since 1850 have had significant browsing impacts in the alpine vegetation of Northwest Nelson. *Fuscospora cliffortioides* is the most conspicuous arboreal species of the treeline of Northwest Nelson and around Adelaide Tarn. Additionally, *Lophozonia menziesii* and *Dacrophyllum traversii* are the other trees most commonly found near the treeline, while several species of the genera *Coprosma*, *Raukaua* and *Griselinia* are abundant in the sub-canopy treeline forest stands. The herbaceous ground cover of these treeline communities includes a combination of monocotyledonous genera such as *Astelia* and *Uncina*, in association with multiple dicotyledonous groups such as *Anisotome* (Apiaceae), *Ourisia* (Plantaginaceae) and *Lagenophora* (Asteraceae).

A 0.5–3.0-m-tall shrubland community dominated by *Olearia colensoi* and *Dacrophyllum uniflorum* is usually found above the treeline of the Douglas mountain range (Fig. 1). Other shrub species include *Halocarpus biformis*, *Brachyglottis bidwillii*, *Gaultheria crassa*, *Hebe albicans* and several species of the genus *Coprosma*. This shrubland community may extend up to ~1500 m in sunny and well-drained bedrock ridges or hillslopes, where it is usually superseded by tussock grassland formed by several species of the genus *Chionochloa*. In the few mountainous areas above 1500 m, these tussocklands usually give way to open grassland areas with scattered patches of *Oreobolus pectinatus* cushionfields and patches of *Helichrysum intermedium* and *Hebe ciliolata*. These open cushionfield and grass patches represent the limit of the alpine vegetation before giving way to non-vegetated high-alpine colluvium landforms. Vegetation surrounding Adelaide Tarn consists primarily of *Chionochloa* tussock grassland. Additionally, *Hebe biformis* and *Dacrophyllum uniflorum* form dense thickets on scree areas to the east of the site. Approximately 100 m to the north, *Fuscospora cliffortioides* forms a dense treeline boundary on the steep mountain slopes. Restiads, primarily *Empodisma minus* and *Carex* spp., are prominent in the boggy margins of Adelaide Tarn, while aquatic plants *Potamogeton* (probably *P. cheesemanii*) and *Isoetes* spp. grow in the shallow muddy margins (Marcus J. Vandergoes, pers. obs.).

Methods

Sediment retrieval

We obtained two overlapping sediment cores (AT 1115 and AT 1116) taken from an anchored platform at the deepest part of Adelaide Tarn (water depth ~7 m). Each core comprises multiple 1-m length sections retrieved with a 5-cm-diameter square-rod piston corer (Wright, 1967). The two series showed the same stratigraphic units, thus enabling a single site composite sequence to be constructed devoid of any break between individual core segments. Additionally, we obtained a gravity core to retrieve the water–sediment interface. The replication of stratigraphic features in the gravity and overlapping cores allowed us to construct a single site sequence (hereafter referred to as a single core) that extends continuously up to the present.

Stratigraphy and chronology

We described the broad lithological properties of the cores through visual inspection, standard photography and X-ray images after carefully cleaning the core surfaces. The images are not presented here but were used to confirm field-based lithological correlations between the two overlapping core series. Magnetic susceptibility analysis was performed at Victoria University of Wellington using an MS2 Bartington magnetic meter with a sensor type M.S.1C. Grain size analysis was performed on the sub-2-mm-diameter fraction using a Malvern Master sizer 2000 at the University of Waikato, after pre-treatment with H_2O_2 and deflocculation. Data are expressed as percentage of clay (<3.9 μm), silt (3.9–60 μm) and sand (60–2000 μm) with respect to volume units. Grains >2 mm in diameter were not characterized except for gravel layers noted in the lithostratigraphy.

The chronology of the sediment sequence is constrained by 16 accelerator mass spectrometry radiocarbon dates obtained from plant macrofossils. Radiocarbon calibration was performed using the SHCal13 dataset (Hogg *et al.*, 2013) included in the software CALIB 6.01 (Stuiver, 1993). We further produced a Bayesian age–depth model with the aid of the Bacon package using R software (Blaauw and Christen, 2011). This method enabled the calculation of a weighted mean and a 95% confidence interval for the calendar age distribution of every level in the sedimentary sequence, including the individual pollen and plant macrofossil sample layers. The pollen and plant macrofossil data are plotted against their weighted mean calendar age indicated by the model.

Pollen record

We processed and analysed 110 samples extracted from constant volume (1 cm^3), 1-cm-thick sections taken at 5-cm

intervals throughout the core. The sample processing followed standard procedures (Faegri and Iversen, 1989). We counted 300 terrestrial pollen grains from each pollen slide and calculated percentages based on the terrestrial pollen sum along with pollen concentrations and pollen influx (influx: grains cm^{-2} a^{-1}) for individual taxa. The percentages of aquatic pollen, fern spores and tree fern spores were calculated from the sum of all terrestrial pollen taxa plus the respective ecological group. Pollen percentage and influx diagrams were generated with the software Tilia version 2.0 (E. Grimm, Illinois State Museum, Springfield, IL, USA). A pollen zonation was determined based on the visual identification of the main pollen percentage changes, assisted by a stratigraphically constrained ordination (CONISS) provided and executed by the same software.

Plant macrofossil record

The same 110 sample levels used for pollen Analyses were processed for plant macrofossil analyses, although not all samples yielded identifiable material. The sample processing involved separation by wet sieving at 90 μm, and was followed by counting individual specimens with the aid of a square gridded transparent slide under a stereomicroscope. The identification of fossil remains was based on photographic and herbarium references from the University of Waikato.

For the Nothofagaceae leaf fragments that could not be confidently identified from leaf morphology, we isolated the cuticle layer and examined the cellular pattern by light microscopy. The cuticle analysis confirmed the morphology-based identification of all *Lopohozonia menziesii* and *Fuscospora cliffortioides* specimens but showed that the few fragments ascribed to *F. fusca* were instead *L. menziesii*. The category 'Nothofagaceae undifferentiated' refers to leaf fragments that could not be identified beyond family level by these methods. We assume these specimens are either *L. menziesii* or *F. cliffortioides* because only these Nothofagaceae trees occur at treeline altitude today and only these two Nothofagaceae species have been positively identified in the macrofossil assemblages.

Fragments of grass, sedge and rush stems dominated the macrofossil assemblages but could not be taxonomically separated and so were recorded as 'graminoid'. To counter the problem of quantifying fragments, a transformation was applied in which eight fragments equated to one complete unit. Macrofossil data are expressed with the aid of a relative abundance scale as follows: (1) rare, (2) uncommon, (3) frequent, (4) common, (5) abundant.

As the site elevation falls within the regional limits of the present-day treeline, a long-term absence of arboreal macroscopic plant remains will be interpreted as a lowering of the treeline, and the presence of these remains as the occurrence of treeline around and/or above the site.

Temperature reconstructions

We estimated the thermal changes around Adelaide Tarn by developing three different temperature reconstructions from the pollen data. Two of those reconstructions are quantitative, obtained using the transfer function approach and applying both the (i) partial least squares regression and (ii) modern analogue technique to the New Zealand pre-deforestation pollen dataset (Wilmshurst *et al.*, 2007). Alternatively, a temperature reconstruction was calculated from a pollen–temperature proxy (PTP) using individual taxa with well-established thermal affinities that are prominent in the Adelaide Tarn record. The PTP is calculated as the normalized base-10 logarithm of the ratio of *D. cupressinum* + *Prumnopitys taxifolia* + *P. ferruginea* pollen influx to the combined pollen influxes of *Lophozonia* + total grasses. All these taxa are prominent through most of the Adelaide Tarn pollen record, and are broadly representative of their respective vegetation communities with temperature-controlled altitudinal patterns observed in the region today. We exclude the taxon *Fuscospora* as it includes species found from low to subalpine elevations. The taxa included in the PTP are strongly correlated with mean annual temperature (MAT) in the New Zealand pre-deforestation database (Table 1), and as expected the PTP index shows a strong positive correlation with MAT (correlation coefficient = 0.58; $p < 0.001$) in the same dataset (Fig. S1 in the supplementary information). Thus, positive (negative) values of PTP indicate the relative dominance (subordination) of the more thermophilous *D. cupressinum* and/or *Prumnopitys* spp. over the other, cool indicator taxa under relatively warm (cold) conditions.

Results

Stratigraphy and chronology

The sediment core features sand and gravel units at their base of the cores. The sequence has a total length of 570 cm and is dominated by organic silts (relative average abundance = 51%) and clays (45%), with a minor content of sands (4%). We recognize three main sedimentary units (Fig. 3):

1. The lower unit (560–480 cm) comprises inorganic grey silts and clays. The basal portion of this unit features thin (~1 cm thick) inorganic laminae and three prominent (>2 cm thick) gravel layers. A yellowish silt layer is evident at 494–493 cm.

2. The middle unit (479–238 cm) comprises brownish black silt and clay units with abundant macrofossils in its upper portion. Organic laminae occur and yellowish silt layers are particularly abundant. A gravel layer is observed between 391 and 389 cm.

3. The upper unit (237–1 cm) comprises organic-rich dark brown silt and clay with abundant diatoms and macroscopic remains. Additionally, horizontal yellowish silt layers and a series of organic-rich laminae containing liverworts, mosses and unidentifiable concentrations of macrofossils are observed at various levels.

All calibrated radiocarbon ages are in chronological order (Fig. 3; Table 2) which, together with the absence of any stratigraphic and visual evidence for significant break or disruption in the sedimentary sequence above the uppermost gravel layer at ~12.5k cal a BP (11 464 ± 40 ^{14}C a BP), suggests that sediment accumulation was essentially continuous since that time. Because macroscopic organic material is absent from the lower unit, the oldest radiocarbon date was obtained at a depth of 463 cm (570 cm of total depth), and the chronology below this point has been determined by extrapolation. The Bayesian age model derived from the

Table 1. Spearman rank correlation *r*-values for key Adelaide Tarn taxa in the New Zealand pre-deforestation pollen database versus mean annual temperature (MAT). All correlations shown are significant at $P = 0.05$. Data from Wilmshurst *et al.* (2007).

Taxon	Correlation with MAT	Rank out of all taxa ($n = 82$)
Dacrydium cupressinum	0.51	5th most thermophilous
Poaceae	−0.49	4th least thermophilous
Lophozonia menziesii	−0.51	3rd least thermophilous

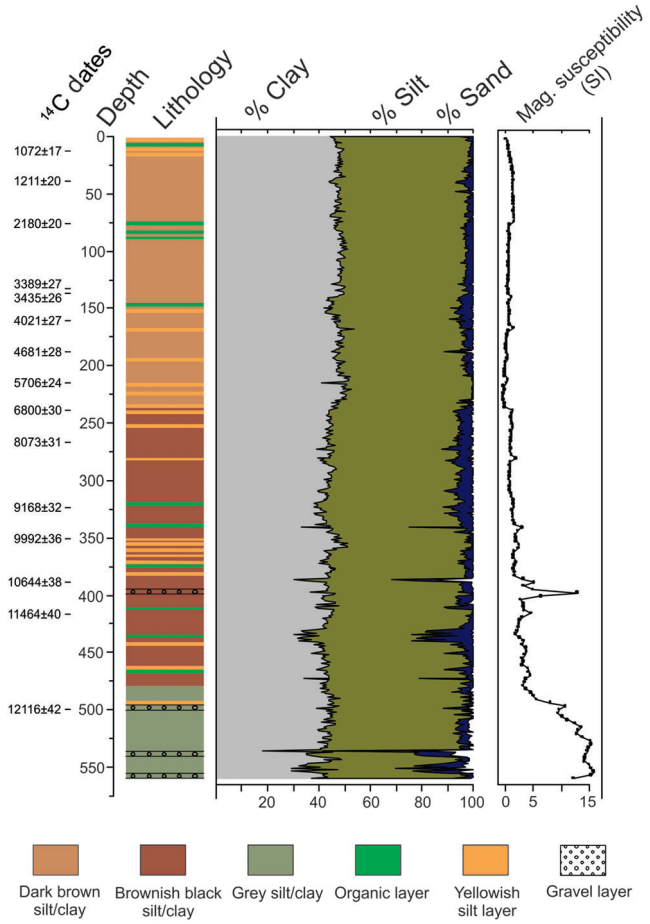

Figure 3. Radiocarbon ages (^{14}C a BP, ± 1 SD), lithology, grain size and magnetic susceptibility analyses of the correlated sediment section retrieved from Adelaide Tarn.

calibrated ages (Fig. 4) indicates sediment accumulation rates ranging from 9 to 98 years cm^{-1} with an average of 28 years cm^{-1}. The average time resolution of the pollen record is 147 years per sample. The weighted average for the maximal extrapolated age of the sequence is 16.1k cal a BP (95% confidence range = 15.4–16.9k cal a BP) and the maximal age for the pollen record is 15.8k cal a BP (15.2–16.6k cal a BP).

Pollen record

We divided the pollen percentage record of Adelaide Tarn into six zones based on key changes observed in pollen composition and the CONISS ordinations. The main features of each zone are described in Table 3. Both pollen percentages (Fig. 5) and influx (Fig. 6) are presented.

In summary, the pollen record shows the overall dominance of tree pollen (average 65%) over grass (18%) and shrub (13%) pollen. The most common taxon is *Fuscospora*, which has maximum abundance at the beginning of the record between 15.8 and 14.8k cal a BP, and later during the last 7000 years. In the interim, a series of other pollen taxa show significant changes in their abundance, starting with an interval of high shrub and grass abundance between 14.8 and 12.5 k cal a BP and followed by an increase in low- and mid-elevation conifers between 12.5 and 8.5k cal a BP (Fig. 5).

Plant macrofossil record

We distinguished three distinctive zones in the plant macrofossil record of Adelaide Tarn (Fig. 7). The lower zone, between 15.8 and 9.8k cal a BP, is exclusively dominated by graminoids and bryophytes with their abundances ranging from rare to frequent. The appearance of *Lophozonia menziesii* at 9.7k cal a BP represents the first arboreal presence in the record and marks the beginning of the middle zone. *L. menziesii* abundance ranges from rare to uncommon between 9.7 and 3k cal a BP, while *Fuscospora cliffortioides* ranges from rare to abundant across approximately the same time interval. Leaves of *Libocedrus bidwillii* are present but rare between 9.3 and 8.8k cal a BP. Between 9.7 and 2.7k cal a BP, graminoid and bryophyte abundances remain stable with values ranging from rare to uncommon. The upper zone spans the last 2700 years when the abundance of tree taxa declines significantly except for isolated appearances of rare *L. bidwillii*, whereas graminoid and bryophyte abundance remains comparatively stable throughout.

Temperature reconstructions

In broad terms, the temperature curves derived from the two different quantitative reconstructions (partial least squares and modern analogue technique) show similar long-term trends with MATs ranging between 6.0 and 8.5 °C (Fig. S2). The main difference between the two curves is a marked cooling

Table 2. Summary of the radiocarbon dates from Adelaide Tarn.

No.	Laboratory code (CAMS no.)	Correlated length (cm)	^{14}C date ± 1σ (years)	Calibration curve	Lowest 2σ intercept (cal a BP)	Upper 2σ intercept range (cal a BP)	Oldest–youngest difference	Median probability (cal a BP)
1	NZA51077	13	1072 ± 17	SHCal13	927	955	28	941
2	NZA999	37	1211 ± 20	SHCal13	989	1092	103	1066
3	NZA998	75	2180 ± 20	SHCal13	2086	2281	195	2126
4	NZA37637	83	2467 ± 25	SHCal13	2359	2652	293	2459
5	NZA50821	133	3389 ± 27	SHCal13	3514	3637	123	3586
6	NZA50822	137	3435 ± 26	SHCal13	3591	3687	96	3637
7	NZA50823	161	4021 ± 27	SHCal13	4417	4514	97	4463
8	NZA50824	188	4681 ± 28	SHCal13	5314	5447	133	5406
9	NZA50905	215	5706 ± 24	SHCal13	6408	6473	65	6444
10	NZA50825	239	6800 ± 30	SHCal13	7582	7653	71	7614
11	NZA51059	267	8073 ± 31	SHCal13	8785	8887	102	8900
12	NZA51060	324	9168 ± 32	SHCal13	10 228	10 367	139	10 268
13	NZA50826	351	9992 ± 36	SHCal13	11 254	11 403	149	11 357
14	NZA50829	389	10 644 ± 38	SHCal13	12 557	12 646	89	12 596
15	NZA50827	417	11 464 ± 40	SHCal13	13 202	13 311	109	13 259
16	NZA50828	463	12 116 ± 42	SHCal13	13 823	14 000	177	13 917

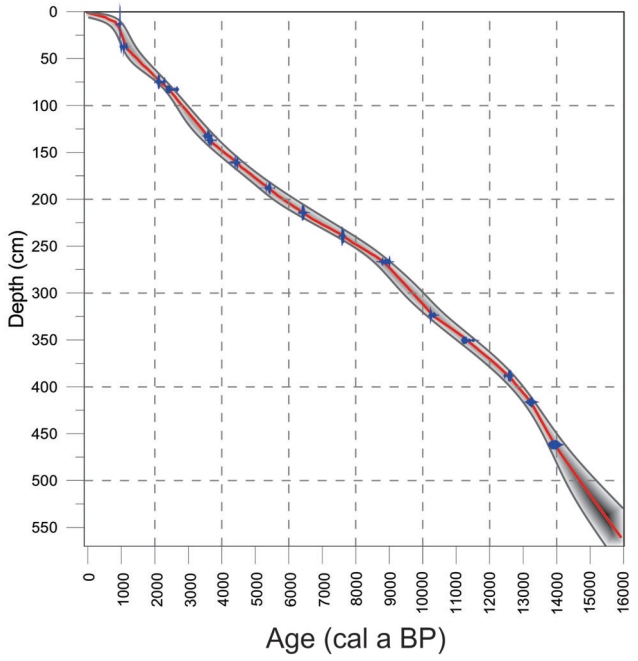

Figure 4. Bayesian age model based on the 16 radiocarbon dates from Adelaide Tarn. The model was developed using the Bacon package for the software R (Blaauw and Christen, 2011). Radiocarbon calibration was performed with the aid of the software CALIB 6.01 (Stuiver, 1993) using the SHCal13 calibration curve (Hogg *et al.*, 2013). The image shows the 2σ calendar age range for each of the ages (blue), the modelled weighted mean age (red line) and the 95% confidence intervals (grey lines). The darker areas represent calendar ages with a high likelihood according to the model. The weighted mean age series is used to estimate an age for all pollen and plant macrofossil samples.

between 16 and 10k cal a BP shown by the modern analogue technique but not replicated by the partial least squares reconstruction. Both quantitative estimations show persistent warming trends between 10 and 3k cal a BP and no consistent trends after this interval. In contrast, the qualitative PTP shows marked warming pulses between 14.8–10 and 7–6k cal a BP and cooling trends between 10 and 7 k cal a BP and over the last 3000 years.

Discussion

Patterns of vegetation and climate change at Adelaide Tarn

The Adelaide Tarn pollen, plant macrofossil and sedimentological records provide a well-resolved history of vegetation and catchment conditions for the last ~15 800 years (Figs 5–7). Previous work has shown that pollen sites in this high-altitude setting are sensitive not just to the vegetation communities at that elevation, but also to those growing on lower slopes (Moar, 1970; McGlone and Basher, 2012) so they can provide insight into climate-related changes in altitudinal vegetation across a broad elevation range.

Between the extrapolated ages of 15.8 and 14.8k cal a BP the pollen record is characterized by high levels of the forest tree taxon *Fuscospora*, the shrub-small trees *Phyllocladus*, *Coprosma* and *Myrsine*, and herb pollen. In contrast, the plant macrofossil record shows only non-arboreal taxa (Fig. 7), suggesting local dominance of alpine grassland and a lowered treeline under relatively low temperatures. Cold conditions are also suggested by the low organic productivity, as indicated by the absence of organic brown sediments in the lake at that interval. The differences between the pollen and plant macrofossil records can be reconciled by considering that the pollen of *Fuscospora* and the other woody sub-alpine taxa were probably wind-transported both inland and upslope from distant sources across a relatively open landscape, a feature that has been observed in modern pollen rain studies (Bussell, 1988; McGlone and Basher, 2012). Potential sources of *Fuscospora* trees include the coastal regions of north-west South Island, to the west and south-west of the study site, where Last Glacial Maximum pollen assemblages dominated by *Fuscospora* (up to 80%) have been reported (Moar *et al.*, 2008; Newnham *et al.*, 2013). Further support for this interpretation comes from the comparatively low terrestrial pollen influx observed during this interval (Fig. 6), consistent with sparse local vegetation and open landscape. Such conditions are likely to have existed during the earliest part of the Adelaide Tarn record when local vegetation communities were adjusting to recent deglaciation. The alternative explanation – that southern beech trees were established around the lake at ~14k cal a BP – is not supported by our plant macrofossil evidence or by independent palaeoecological and palaeoclimatic records for this time (e.g. McGlone and Basher, 2012; Barrell *et al.*, 2013).

Between 14.8 and 12.5k cal a BP, *Fuscospora* declines rapidly from ~55 to ~25%, accompanied by a steady increase of *Lophozonia menziesii* and the appearance of several representatives of the conifer–broadleaf forest. During this period, herbs including Apiaceae, *Astelia* and Poaceae show significant expansions (Fig. 5) while a lithological transition from the inorganic grey unit to a darker organic brownish black silt/clay occurs at 14.3k cal a BP (Fig. 3). There is still no trace of any arboreal elements in the macrofossil record (Fig. 7), suggesting that a forest-free environment persisted around the lake. Whereas the appearance of conifer–broadleaf taxa and the transition to a darker silt unit suggest a relative climate amelioration, the increments in *Lophozonia* and grass pollen suggest the opposite trend. Total terrestrial pollen influx underwent a five-fold increase from Zone 1 (900 grains cm^{-2} a^{-1}) to Zone 2 (4400 grains cm^{-2} a^{-1}) and all major pollen taxa, including *Fuscospora*, experienced increases in their accumulation rates (Fig. 6). The marked decrease in *Fuscospora* percentages therefore may reflect the proportionate increase of other terrestrial pollen, rather than a major decline in *Fuscospora* trees. The pollen-derived climate signal is therefore ambiguous for this interval, although as discussed in the following sections, our preferred temperature reconstruction shows an attenuation of the warming trend that commenced before that period.

At ~12.5k cal a BP, pollen levels of Poaceae and other herb taxa decline from their previous maxima while percentages of lowland to sub-alpine conifer–broadleaf tree taxa increase substantially. Prominent among these trees is the tall podocarp *Dacrydium cupressinum*, a lowland tree restricted to humid lowland areas below 600 m (Franklin, 1968). These increments suggest that conifer–broadleaf forest with prominent *D. cupressinum* expanded upslope to attain its present upper altitudinal limits or higher. Judging by the *D. cupressinum* curve (Fig. 5), peak elevation may have been reached by 10k cal a BP, close to the time that tree macrofossils first appear at Adelaide Tarn. We conclude that, from 12.5k cal a BP and possibly earlier, forest communities expanded upslope across the region as a response to sustained warming.

Fuscospora pollen abundances began to increase between 9.8 and 7k cal a BP, along with the sub-alpine taxon *Halocarpus*, when other lowland to montane trees including *D. cupressinum* decline. This change signals the curtailment of the previous warming trend, although a plateau of

Table 3. Summary of Adelaide Tarn pollen zones.

Zone	No. of samples	Stratigraphic position (cm)	Age range (cal a BP)	Dominant taxa (zone mean)	Additional information
AT 1	9	507–557	14 800–15 800	*Fuscospora* (52%), *Phylocladus* (11%), Poaceae (11%)	Minor contributions of *Lophozonia menziesii*, *Coprosma* and Asteraceae. High total tree percentages and low shrub percentages.
AT 2	25	387–502	12 500–14 800	*Fuscospora* (25%), Poaceae (17%), *Phylloladus* (14%)	Abrupt drop of *Fuscospora* and increments in *L. menziesii*, *Prumnopitys taxifolia* and *Libocedrus*. Grassland taxa Apiaceae, *Astelia* and Poaceae reaching their record maxima, making the total tree percentage drop significantly
AT 3	13	313–382	10 000–12 500	Poaceae (14%), *Lophozonia menziesii* (13%), *Fuscospora* (12%)	*Fuscospora* reaches minimum abundances while *L. menziesii* continues its increasing trend. *Dacrydium cupressinum* experiences a significant increase throughout. Conifer–broadleaf taxa including *P. ferruginea*, *P. taxifolia* (6%), *Libocedrus* and *Metrosideros* increase notably. Poaceae, *Astelia*, Apiaceae and Asteraceae show overall diminution.
AT 4	10	263–308	8700–10 000	*Dacrydium cupressinum* (15%), *Lophozonia menziesii* (14%), *Fuscospora* (14%)	*Fuscospora* recovers from minima while *L. menziesii* high ambundances persist. *D. cupressinum* reaches a peak plateau. *Prumnopitys ferruginea*, *P. taxifolia*, *Libocedrus* and *Metrosideros* decrease with respect to the previous zone, while the shrub conifer *Halocarpus* shows a notable increment. All grass taxa decline in this zone
AT 5	10	213–258	6400–8700	*Fuscospora* (32%), *Lophozonia menziesii* (13%), *Dacrydium* (10%)	*Fuscospora* continues recovering while *D. cupressinum* starts to decline. *P. ferruginea*, *P. taxifolia*, *Libocedrus* and *Metrocideros* show minimal abundances and *Halocarpus* declines considerable. The total shrub and herb abundances show considerable diminutions. Notably, this zone features a significant increment in the littoral macrophyte *Isoetes* (increment from 2 to 10%).
AT 6	43	1–208	Present to 6400	*Fuscospora* (49%), *Isoetes* (15.7), *Lophozonia menziesii* (10%)	Stable high abundances of *Fuscospora*, *L. menziesii* and *D. cupressinum* (9%) are the main features of this zone. Almost all the conifer–broadleaf taxa show minimal abundances, except *Halocarpus* which shows a gentle recovery. Total shrubs and herbs do not show major changes, while *Isoetes* shows high-magnitude oscillations superimposed on an increasing trend. No exotic pollen is found in this or any previous zone.

relatively high abundance of *D. cupressinum* until 7.6k cal a BP indicates the persistence of comparatively mild and moist conditions. The plant macrofossil record shows the appearance of *Libocedrus bidwillii* together with *Fuscospora cliffortioides* and *Lophozonia* leaves. *L. bidwilii* is a conifer with a broad altitudinal range and is a common floristic element of lowland and montane conifer–broadleaf forest communities. However, its association with *L. menziesii* and *F. cliffortioides* occurs mainly above 700 m in the western South Island (Veblen and Stewart, 1982), and therefore their

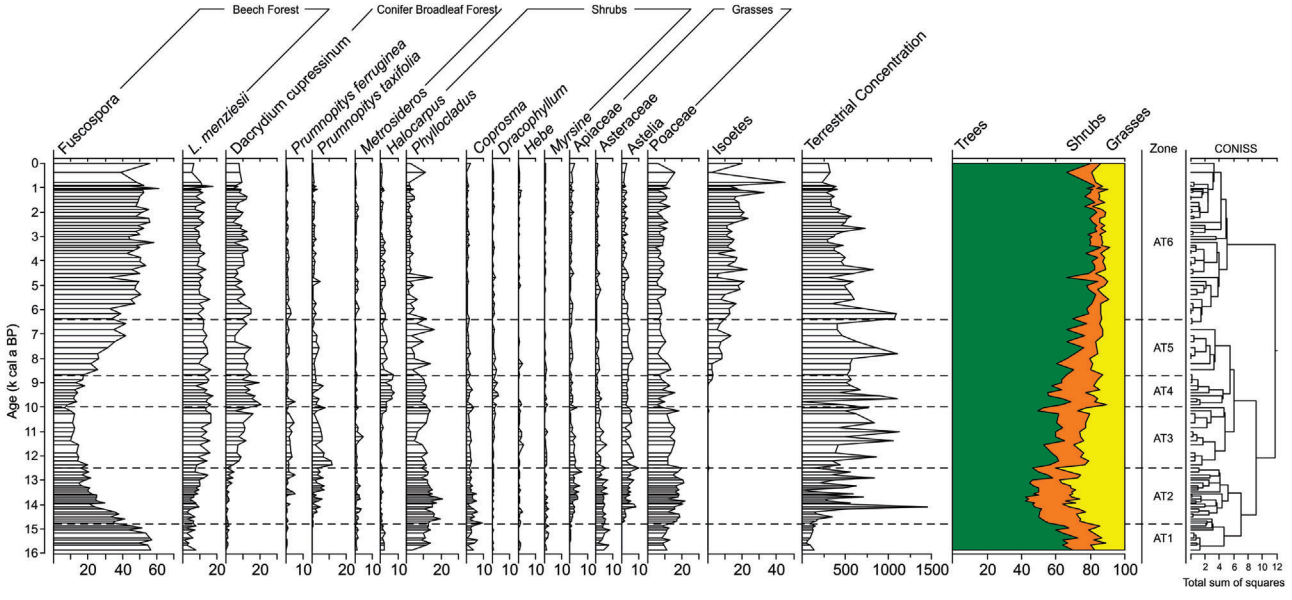

Figure 5. Adelaide Tarn pollen percentage diagram. Percentage changes of the main pollen taxa are plotted against the time scale obtained from the age model. The diagram includes the total concentration of terrestrial pollen and the total sum of trees, shrubs and grass taxa, as well as a stratigraphically constrained zonation of the pollen data using the statistic tool CONNISS.

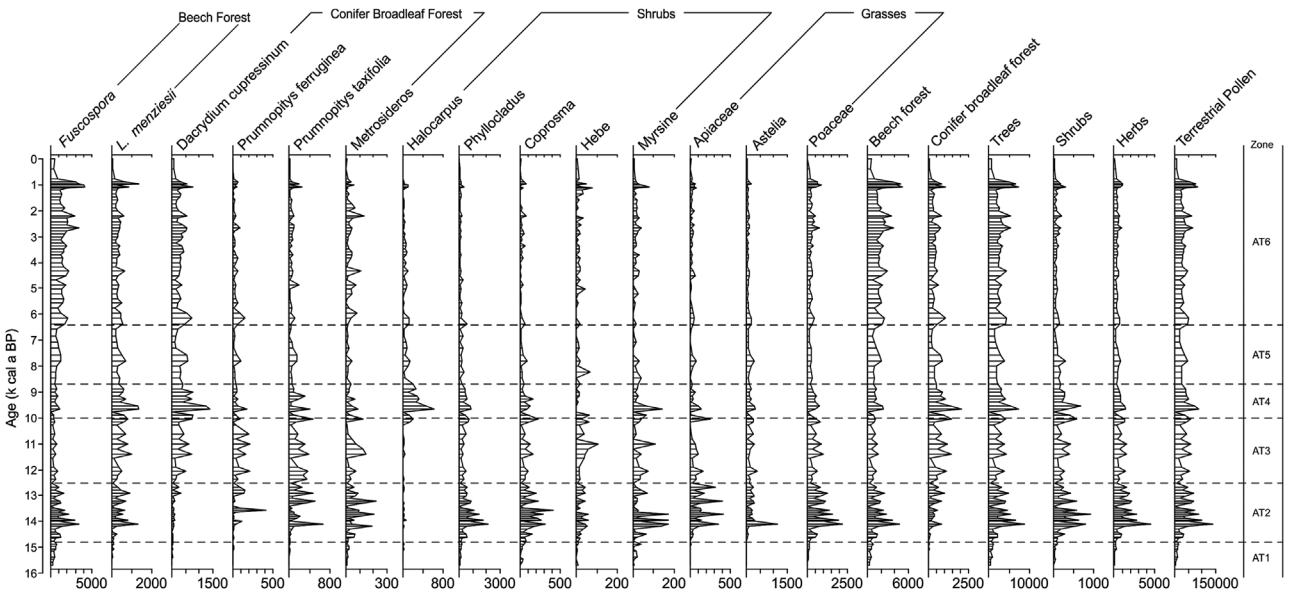

Figure 6. Adelaide Tarn pollen influx diagram. Pollen influx (grains cm^{-2} a^{-1}) is plotted against the weighted mean calendar age indicated by the age model. The diagram includes the total influx of trees, shrubs and grasses, as well as the sum of beech and conifer broadleaf forest taxa. Note that all values are divided by 100 except the values of *Fuscospora*, total Trees, Herbs, total Terrestrial pollen, which are divided by 1000.

coexistence in the macrofossil record suggests a local development of high-elevation southern beech forest with minor presence of conifers, a similar vegetation pattern to that near the lake today. The increase in *Fuscospora* pollen therefore suggests the local establishment of *Fuscospora cliffortioides* trees. Although the overall decrease in the percentages of lowland to montane trees could be associated with a masking effect of the increase of local *Fuscospora* pollen, the influx of these former taxa decreases notably after 9k cal a BP (Fig. 6), suggesting a genuine decline. Additionally, a lithostratigraphic change from dark brown to light brown clay/silt sediment at 7.6k cal a BP (Fig. 3) suggests a decrease in the organic productivity of the lake as a response to lower temperatures. We therefore suggest a contraction of the conifer–broadleaf forest community in response to an overall cooling trend between 10 and 7k cal a BP, although this trend lacked the intensity or continuity to push the treeline below the Adelaide Tarn basin. This pollen–climate trend is more marked between 7.6 and 7k cal a BP and subsequently reversed between 7 and 6k cal a BP with an increase in *D. cupressinum* and a plateau of *Fuscospora*.

After ~6000 cal a BP, *Fuscospora* pollen increased steadily again through to the present while most other terrestrial taxa remain relatively constant (Fig. 5). The macrofossil record indicates the continuing presence of the tree taxa *Fusospora cliffortioides*, *Lophozonia menziesii* and *Libocedrus bidwillii* around the site during the mid- and late Holocene (Fig. 7). At ~ 2.7k cal a BP there is a major change, with the disappearance of most trees from the macrofossil record. This event suggests a lowering of the treeline in response to a cooling trend starting at 2.7k cal a BP or before.

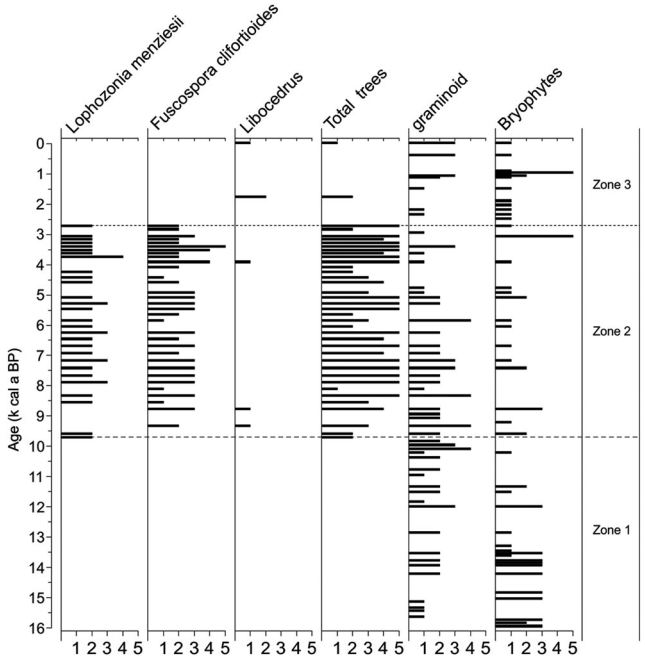

Figure 7. The Adelaide Tarn plant macrofossil record showing the major species identified and their variation with respect to a relative abundance scale: (1) rare, (2) some, (3) many, (4) common and (5) abundant.

Regional palaeoclimate implications

A Lateglacial cooling interval, broadly corresponding to the Antarctic Cold Reversal (14.5–12.8k cal a BP), has been recognized in palaeoecological (Newnham and Lowe, 2000; Vandergoes *et al.*, 2008; Lowe *et al.*, 2013), glacial (Putnam *et al.*, 2010; Kaplan *et al.*, 2013) and speleothem (Hellstrom *et al.*, 1998) records from New Zealand (see also Alloway *et al.*, 2007; Barrell *et al.*, 2013). The climate signal at Adelaide Tarn is ambiguous for this period in that both cool and warm climate indicators are observed. In particular, an increase in the abundance of alpine herbs is especially evident between 13.7 and 13k cal a BP and implies cooler conditions at the site, whereas a minor increase in the lowland–montane tree taxon *Prumnopitys* implies warming at lower elevations. Interpretation of these signals is complicated by local site factors as the catchment vegetation and hydrology were likely to be still adjusting to recent glacial retreat and by the changing 'masking' effect of the predominant pollen taxon during this zone, *Fuscospora*. Therefore, we refrain from conclusive assertions about this interval.

In contrast, unambiguous evidence for warming at Adelaide Tarn between 12.5 and 9.8k cal a BP is consistent with the assertion of an early Holocene (11.5–9k cal a BP) warm event widespread in New Zealand (Williams *et al.*,

2005; McGlone and Moar 1977; McGlone *et al.*, 2004; McGlone *et al.*, 2011). From a comparison of pollen and macrofossil data with a forest simulation model, McGlone *et al.* (2011) suggested that MATs in the central South Island between 11.5 and 9.5k cal a BP were at least 1.5 °C higher than present, although they also indicated that summers could have been cooler and precipitation reduced by at least 30%. Vegetation patterns at this time were attributed to a combination of reduced seasonal extremes in temperature, warm oceans and reduced westerly wind flow. The argument of McGlone *et al.* (2011) for colder summers despite overall higher annual temperatures is supported by a series of records from sites at the present treeline that show minimal or no forest during the early Holocene. The plant macrofossil record at Adelaide Tarn, situated just below the modern treeline, is consistent with this scenario because the first unequivocal evidence for establishment of a treeline at this elevation is not observed until 9.7k cal a BP, towards the end of this early Holocene warming interval. However, we acknowledge that the relatively late appearance of arboreal elements in the plant macrofossil record might also be the result of slow tree migration rates and not necessarily from cooler summers.

Adelaide Tarn temperature proxies

The quantitative pollen–temperature reconstructions derived for Adelaide Tarn using the modern analogue technique and partial least squares approaches differ fundamentally from that derived using the PTP index (Fig. S2). We question the applicability of both quantitative temperature reconstructions in light of these differences and several other observations (see supplementary information). The quantitative temperature reconstructions are also fundamentally at odds with many of the temperature inferences drawn from the pollen and plan macrofossil records discussed above. In particular, the earliest part of the record (16–14k cal a BP) is shown as warmer than most of the interval 12–9k cal a BP; and the late Holocene is shown as warmer than the early Holocene. Previous work (Wilmshurst *et al.*, 2007; Newnham *et al.*, 2013) has highlighted problems with the New Zealand pollen–climate transfer function approach when applied to cold climate reconstructions due to limitations in the modern training set. Further complications arise from the distorting influence of *Fuscospora*, a commonly over-represented and widely dispersed pollen type with an ambiguous temperature affinity. The qualitative PTP reconstruction, on the other hand, avoids both these limitations since it has been developed in the context of the known regional vegetation–climate relationships and is strongly correlated with MATs in the pre-deforestation pollen dataset (Fig. S1). Although the PTP index is qualitative, we conclude that it can be used as a reliable temperature proxy at this site. We now turn to a comparison of other Southern Hemisphere climate records using the Adelaide Tarn PTP index.

Links with millennial-scale low- and high-latitude climate variations

The Adelaide Tarn PTP shows a pause in an ongoing warming trend between 13.7 and 13k cal a BP (Fig. 8). This pause overlaps with the later part of the Antarctic Cold Reversal and with a stalling or slight decline of the deglacial increase in global atmospheric CO_2 concentrations (EPICA community members 2004; Monnin *et al.*, 2004; Fig. 8). As the main source of cold and moist air masses in the Northwest Nelson region is the southern westerly wind (SWW) belt, then the implication for this attenuation at Adelaide Tarn is that the prevailing westerly circulation was positioned further northwards from its current position and consequently intensified at Adelaide Tarn. We emphasize that this particular assertion is tentative due to the difficulties in interpreting the early part of the Adelaide Tarn pollen record noted earlier.

A warming trend observed in the PTP index between 12.5 and 10k cal a BP (Fig. 8), also observed elsewhere in New Zealand as discussed earlier, implies a weakening of the westerly circulation over Northwest Nelson because of a southward migration of the SWW belt. The warming trend includes a rapid phase between 13 and 12k cal a BP and a plateau between 12 and 10k cal a BP, and is well aligned with a rapid increase in Antarctic temperature between 12.5 and 11.5k cal a BP and a peak warming between 11.5 and 9k cal a BP. These patterns at Adelaide Tarn concur with relatively high temperatures recorded in ocean records in the western margin of the Antarctic Peninsula (64°S) (Shevenell *et al.*, 2011) as well as trends in global atmospheric CO_2 measured in Antarctic ice cores (Monnin *et al.*, 2004; Fig. 8).

Further temperature co-variations between Adelaide Tarn and the Antarctic/Southern Ocean sector are evident in the form of: (i) a cooling trend accompanied by decreasing atmospheric CO_2 between 10 and 7k cal a BP, and (ii) a less intense warming in both these regions and increasing atmospheric CO_2 between 7 and 6k cal a BP (Fig. 8). The match between the Adelaide Tarn PTP index, Antarctica and the Southern Ocean records represents solid evidence for a continuing teleconnection between the high- and mid-latitudes of the Southern Hemisphere during the late glacial and early Holocene, an inference supported by the strong imprint of Antarctic temperature variability interpreted in pre-Holocene records from the South Island, New Zealand (Vandergoes *et al.*, 2005; Vandergoes *et al.*, 2008; Newnham *et al.*, 2012).

These co-varying temperature changes across the mid/high latitudes probably involved coupled ocean–atmospheric interactions modulated by latitudinal shifts of the SWW belt (Toggweiler *et al.*, 2006; Moreno *et al.*, 2010; Putnam *et al.*, 2010). In this regard, warming intervals between 13 and 10k cal a BP and between 7 and 6k cal a BP in Northwest Nelson could have resulted from a significant reduction of the cold westerly air masses driven by a southward shift of the SWW belt, thereby increasing wind stress over the Southern Ocean around 60°S. Such a shift would have strengthened the Antarctic Circumpolar Current and stimulated the wind-driven upwelling of warmer circumpolar deep waters, warming the Southern Ocean, including the Antarctic Peninsula and promoting ocean CO_2 degasification (Toggweiler and Russell, 2008; Shevenell *et al.*, 2011). Conversely, a northward migration of the SWW belt could have induced the opposite series of events, resulting in a relative cooling around Adelaide Tarn and the Antarctic margin and decrease in CO_2 concentration during the Antarctic Cold Reversal and, to a lesser degree, between 10 and 7k cal a BP.

To some extent the teleconnections between mid- and high latitudes via south/north shifts of the SWW belt proposed here resemble the present-day climate variations expressed by the Southern Annular Mode (SAM). During persistent positive phases of the SAM, the westerly circulation weakens in the mid-latitudes and strengthens in the high latitudes, resulting in a significant warming in New Zealand (Kidston *et al.*, 2009; Fig. 2), Patagonia (Garreaud *et al.*, 2009) and the Antarctic Peninsula (Gillett *et al.*, 2006), while most of the Antarctic mainland cools (Turner *et al.*, 2005). Abram *et al.* (2014) showed this same set of temperature anomalies in their

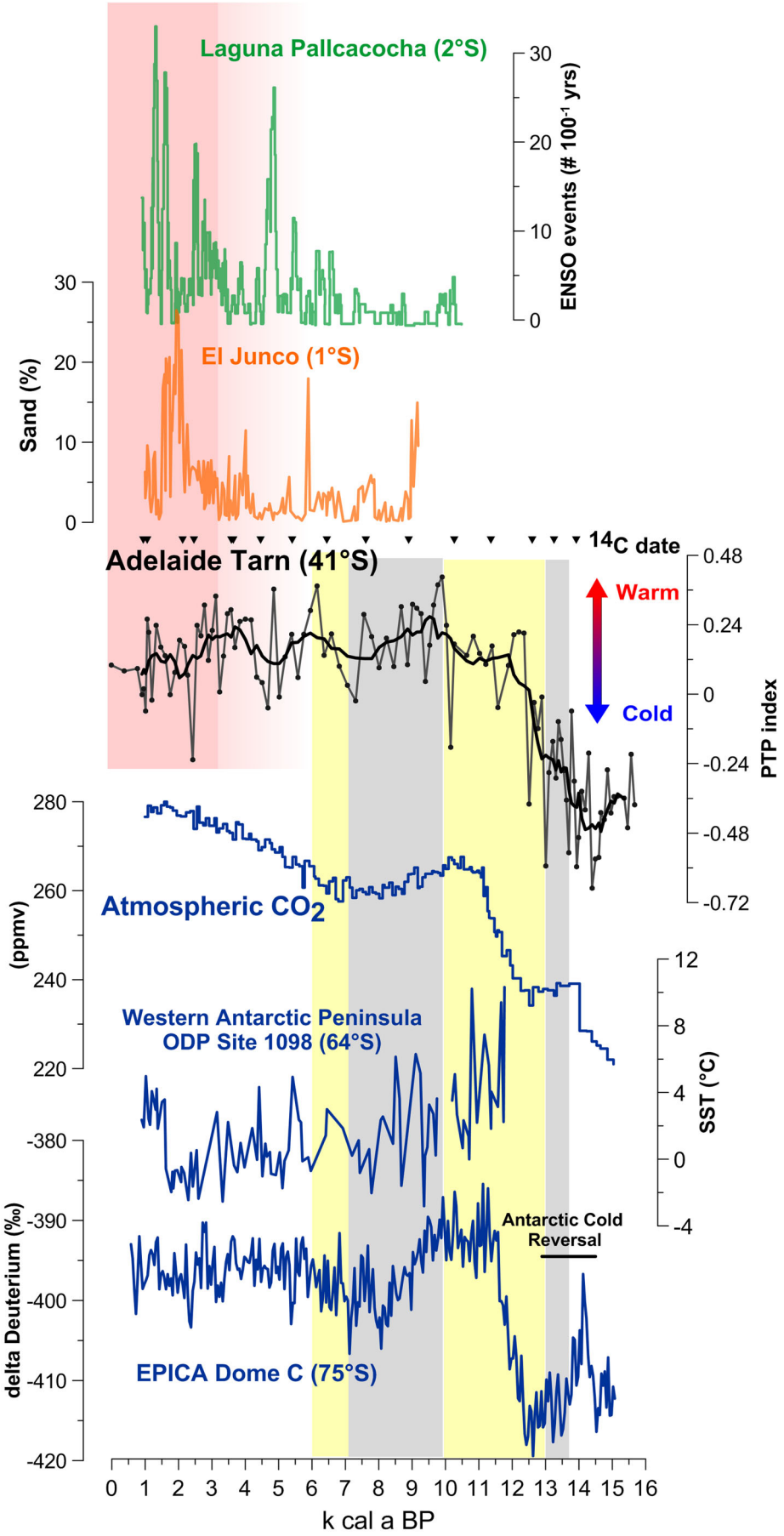

Figure 8. Adelaide Tarn PTP reconstruction (black curve) including all radiocarbon dates (black triangles) compared with climate proxies from the tropical Pacific (above; Moy *et al.*, 2002; Conroy *et al.*, 2008), the global atmospheric CO_2 concentration (Monnin *et al.*, 2004) the Antarctic Peninsula (Shevenell *et al.*, 2011) and east Antarctica (EPICA Community Members, 2004). The grey rectangles indicate cooling or temperature ameliorations; while yellow rectangles indicate warming periods at Adelaide Tarn. The red rectangles indicate periods of relative increased frequency/intensity of El Niño events.

reconstruction of the SAM over the last millennium, which included a sustained positive trend since the 15th century. The millennial-scale warming observed in New Zealand, Patagonia and the Antarctic Peninsula during the early Holocene (13-10k cal yr BP) is consistent with an overall weakening of the westerly circulation in the mid-latitudes. However, the main difference between the present-day spatial pattern of temperature associated with a positive SAM

and the pattern observed during the early Holocene is the intense millennial-scale warming experienced in mainland Antarctica between 12.5 and 9k cal a BP (Fig. 8). One plausible explanation is that high Antarctic temperatures resulted from significantly longer summer duration between 12 and 8k cal a BP. Because summer duration exerts a dominant influence on Antarctic temperature at orbital timescales (Huybers and Denton, 2008), longer Antarctic summers during the first part of the Holocene could have overridden any cooling forcing associated with a positive SAM-like scenario. Thus, although there are some differences between the present-day spatial pattern of temperature anomalies associated with the SAM and the pattern observed during the early Holocene that may arise from differences in orbital configurations, the proxy evidence is still consistent with extended periods of atmospheric circulation analogous to the positive phase of the SAM, and to the negative phase of the SAM between 9.5 and 7.5k cal a BP.

The Adelaide Tarn PTP shows high-magnitude oscillations between 6 and 3k cal a BP and a sustained cooling during the last 3000 years. This latter signal is supported by the plant macrofossil record, yet it is not evident in the temperatures records of EPICA Dome C and the Antarctic Peninsula, which both show centennial-scale oscillations without a consistent longer-term trend. Moreover, the atmospheric CO_2 concentrations show a reversal of the previously declining trend from 7.5k cal a BP onwards and then a long-term steady rise for the remainder of the Holocene. Thus, a breakdown of the early Holocene millennial-scale coupling between Adelaide Tarn and the high-latitude proxies and their correspondence to global atmospheric CO_2 concentration seems evident. One potential mechanism explaining this disconnection emerges when the Adelaide Tarn temperature reconstruction is compared with climate proxies from the tropical Pacific (Fig. 8; Moy *et al.*, 2002; Conroy *et al.*, 2008). These low-latitude proxies suggest an increase in the frequency of El Niño events over the last 4000–5000 years, a trend that has been detected in Holocene lacustrine sediments from northern New Zealand (Gomez *et al.*, 2013). Because present-day El Niño years are associated with a north-eastern displacement of the South Pacific Convergence Zone and an increase in cool westerly and south-westerly flow over New Zealand (Kidson and Renwick, 2002; Fig. 2), more frequent El Niño states during the late Holocene are consistent with a long-term negative temperature trend over New Zealand. We suggest that this trend is discernible in the cooling PTP signal at Adelaide Tarn over the last 3000 years, and in the marked reduction in tree macrofossils from 2.7k cal a BP. Critical to our inference is that the development of frequent El Niño events in the tropical Pacific can explain the downward temperature trend in Adelaide Tarn without necessarily requiring a sustained northward shift of the SWW belt. Such a shift would otherwise be associated with consistent cooling in the Antarctic Peninsula and decreases in atmospheric CO_2, but neither of these trends are observed in high-latitude proxy records (Fig. 8). Stronger climate teleconnections between Adelaide Tarn and the tropical Pacific for the late Holocene are also in agreement with a climate reconstruction from the eastern North Island that shows a switch from a stronger correlation with southern high-latitude records to a stronger influence of tropical Pacific climate by 4.9k cal a BP (Gomez *et al.*, 2012).

Conclusions

Integrated pollen and plant macrofossil records from Adelaide Tarn, a treeline site in mountainous Northwest Nelson, New Zealand, allowed a reconstruction of local and regional changes in vegetation and temperature for the last 16 000 years to be developed. Comparing the millennial-scale temperature trends of this record with other climate reconstructions from New Zealand, Antarctica, the Southern Ocean and the tropical Pacific provides key insights into the evolution of high- and low-latitude climate teleconnections manifested in New Zealand. A tight coupling between the temperature trends in Adelaide Tarn and climate proxies from Antarctica and the Southern Ocean suggests a strong teleconnection with the high latitudes for the interval 15–6k cal a BP, which subsequently weakens. The last 3000 years are marked by a cooling trend in Adelaide Tarn despite rising global atmospheric CO_2 levels, but consistent with other proxy evidence in New Zealand and records of stronger and more frequent El Niño events in the tropical Pacific. This pattern suggest that the Northwest Nelson area developed stronger climate teleconnections with low-latitude ocean–atmospheric circulation systems from the late Holocene onwards. New highly resolved climate reconstructions from New Zealand should test for these changing climate controls, as well as refining their timing and elucidating the precipitation anomalies associated with them. Climate proxies from other terrestrial areas in the Southern Hemisphere mid-latitudes will help to understand the geographical extension of the climate controls proposed here.

Supporting Information

Additional supporting information may be found in the online version of this article.

Figure S1. Pollen diagram showing the relationship between the mean annual temperature (MAT) of 135 pollen sites across New Zealand and their corresponding abundances of selected taxa in the pre-deforestation pollen dataset (see Wilmshurst et al., 2007).

Figure S2. Adelaide Tarn temperature proxies.

Figure S3. The Adelaide Tarn PTP index (without *Fuscospora*) compared with the Northwest Nelson speleothems record (Hellstrom et al., 1998) and the sea surface temperature from the ocean core MD97-2021 (45°S) in the eastern New Zealand Coast (Pahnke and Sachs, 2006).

Acknowledgment. Ignacio A. Jara was supported by Coniciyt Becas Chile. Patricio I. Moreno was supported by Fondecyt grants 1151469 and 1131055, ICM grants P05-002 and NC120066.

Abbreviations. MAT, mean annual temperature; PTP, pollen–temperature proxy; SAM, Southern Annular Mode; SWW, southern westerly wind.

References

Abram NJ, Mulvaney R, Vimeux F *et al.* 2014. Evolution of the Southern Annular Mode during the past millennium. *Nature Climate Change* **4**: 564–569 [DOI: 10.1038/nclimate2235].

Alloway BV, Lowe DJ, Barrell DJA *et al.* 2007. Towards a climate event stratigraphy for New Zealand over the past 30 000 years (NZ-INTIMATE project). *Journal of Quaternary Science* **22**: 9–35 [DOI: 10.1002/jqs.1079].

Barrell DJA, Almond PC, Vandergoes MJ *et al.* 2013. A composite pollen-based stratotype for inter-regional evaluation of climatic events in New Zealand over the past 30,000 years (NZ-INTIMATE project). *Quaternary Science Reviews* **74**: 4–20 [DOI: 10.1016/j.quascirev.2013.04.002].

Blaauw M, Christen JA. 2011. Flexible paleoclimate age-depth models using an autoregressive gamma process. *Bayesian Analysis* **6**: 457–474 [DOI: 10.1214/ba/1339616472].

Bussell MR. 1988. Modern pollen rain, central-western North Island, New Zealand. *New Zealand Journal of Botany* **26**: 297–315 [DOI: 10.1080/0028825X.1988.10410119].

Conroy JL, Overpeck JT, Cole JE *et al*. 2008. Holocene changes in eastern tropical Pacific climate inferred from a Galápagos lake sediment record. *Quaternary Science Reviews* **27**: 1166–1180 [DOI: 10.1016/j.quascirev.2008.02.015].

EPICA_community_member, 2004. Eight glacial cycles from an Antarctic ice core. *Nature* **429**: 623–628.

Faegri K, Iversen J. 1989. *Textbook of Pollen Analysis*, 4th edn. Wiley: New York.

Franklin DA. 1968. Biological flora of New Zealand. *New Zealand Journal of Botany* **6**: 493–513 [DOI: 10.1080/0028825X.1968.10428587].

Garreaud RD, Vuille M, Compagnucci R *et al*. 2009. Present-day South American climate. *Palaeogeography Palaeoclimatology Palaeoecology* **281**: 180–195 [DOI: 10.1016/j.palaeo.2007.10.032].

Gillett NP, Kell TD, Jones PD. 2006. Regional climate impacts of the Southern Annular Mode. *Geophysical Research Letters* **33**: L23704 [DOI: 10.1029/2006GL027721].

Gomez B, Carter L, Orpin AR *et al*. 2012. ENSO/SAM interactions during the middle and late Holocene. *The Holocene* **22**: 23–30 [DOI: 10.1177/0959683611405241].

Gomez B, Carter L, Trustrum NA *et al*. 2013. Coherent rainfall response to middle- and late-Holocene climate variability across the mid-latitude South Pacific. *The Holocene* **23**: 1002–1007 [DOI: 10.1177/0959683613479679].

Hales TC, Roering JJ. 2005. Climate-controlled variations in scree production, Southern Alps, New Zealand. *Geology* **33**: 701–704 [DOI: 10.1130/ G21528.1].

Hellstrom J, McCulloch M, Stone J. 1998. A detailed 31,000-year record of climate and vegetation change, from the isotope geochemistry of two New Zealand speleothems. *Quaternary Research* **50**: 167–178 [DOI: 10.1006/qres.1998.1991].

Hogg AG, Hua Q, Blackwell PG *et al*. 2013. SHCal13 Southern hemisphere calibration, 0-50,000 years cal BP. *Radiocarbon* **55**: 1889–1903 [DOI: 10.2458/azu_js_rc.55.16783].

Huybers P, Denton G. 2008. Antarctic temperature at orbital time-scales controlled by local summer duration. *Nature Geoscience* **1**: 787–792 [DOI: 10.1038/ngeo311].

Kaplan MR, Schaefer JM, Denton GH *et al*. 2013. The anatomy of long-term warming since 15 ka in New Zealand based on net glacier snowline rise. *Geology* **41**: 887–890 [DOI: 10.1130/G34288.1].

Kidson JW, Renwick JA. 2002. Patterns of convection in the tropical pacific and their influence on New Zealand weather. *International Journal of Climatology* **22**: 151–174 [DOI: 10.1002/joc.737].

Kidson JW, Revell MJ, Bhaskaran B *et al*. 2002. Convection patterns in the tropical Pacific and their influence on the atmospheric circulation at higher latitudes. *Journal of Climate* **15**: 137–159 [DOI: 10.1175/1520-0442(2002)015<0137:CPITTP>2.0.CO;2].

Kidston J, Renwick JA, McGregor J. 2009. Hemispheric-scale seasonality of the Southern Annular Mode and impacts on the climate of New Zealand. *Journal of Climate* **22**: 4759–4770 [DOI: 10.1175/2009JC LI2640.1].

Lowe DJ, Blaauw M, Hogg AG *et al*. 2013. Ages of 24 widespread tephras erupted since 30,000 years ago in New Zealand, with re-evaluation of the timing and palaeoclimatic implications of the Lateglacial cool episode recorded at Kaipo bog. *Quaternary Science Reviews* **74**: 170–194 [DOI: 10.1016/j.quascirev.2012.11.022].

McCarthy A, Mackintosh A, Rieser U *et al*. 2008. Mountain glacier chronology from Boulder Lake, New Zealand, indicates MIS 4 and MIS 2 ice advances of similar extent. *Arctic Antarctic and Alpine Research* **40**: 695–708 [DOI: 10.1657/1523-0430(06-111)[MCCARTHY]2.0.CO;2].

McGlone MS, Basher L. 2012. Holocene vegetation change at treeline Cropp Valley, Southern Alps, New Zealand. *Terra Australis* **34**: 343–358.

McGlone MS, Hall GMJ, Wilmshurst JM. 2011. Seasonality in the Early Holocene: extending fossil-based estimates with a forest ecosystem process model. *The Holocene* **21**: 517–526 [DOI: 10.1177/0959683610385717].

McGlone MS, Moar NT. 1977. The Ascarina decline and post-glacial climatic change in New Zealand. *New Zealand Journal of Botany* **15**: 485–489 [DOI: 10.1080/0028825X.1977.10432554].

McGlone MS, Turney CSM, Wilmshurst JM. 2004. Late-glacial and Holocene vegetation and climatic history of the Cass Basin, central South Island, New Zealand. *Quaternary Research* **62**: 267–279 [DOI: 10.1016/j.yqres.2004.09.003].

Moar NT. 1970. Recent pollen spectra from three localities in the South Island, New Zealand. *New Zealand Journal of Botany* **8**: 210–221 [DOI: 10.1080/0028825X.1970.10429121].

Moar N, Suggate RP, Burrows C. 2008. Environments during the Kaihinu Interglacial and Otira Glaciation, coastal north Westland, New Zealand. *New Zealand Journal of Botany* **46**: 49–63 [DOI: 10.1080/00288250809509753].

Monnin E, Steig EJ, Siegenthaler U *et al*. 2004. Evidence for substantial accumulation rate variability in Antarctica during the Holocene, through synchronization of CO_2 in the Taylor Dome, Dome C and DML ice cores. *Earth and Planetary Science Letters* **224**: 45–54 [DOI: 10.1016/j.epsl.2004.05.007].

Moreno PI, Francois JP, Moy CM *et al*. 2010. Covariability of the southern westerlies and atmospheric CO_2 during the Holocene. *Geology* **38**: 727–730 [DOI: 10.1130/ G30962.1].

Moy CM, Seltzer GO, Rodbell DT *et al*. 2002. Variability of El Nino/Southern Oscillation activity at millennial timescales during the Holocene epoch. *Nature* **420**: 162–165 [DOI: 10.1038/nature01194].

Newnham RM, Lowe DJ. 2000. Fine-resolution pollen record of late-glacial climate reversal from New Zealand. *Geology* **28**: 759–762 [DOI: 10.1130/0091-7613(2000)028<0759:FRPROL>2.3.CO;2].

Newnham RM, Lowe DJ, Williams PW. 1999. Quaternary environmental change in New Zealand: a review. *Progress in Physical Geography* **23**: 567–610.

Newnham RM, Vandergoes MJ, Sikes E *et al*. 2012. Does the bipolar seesaw extend to the terrestrial southern mid-latitudes? *Quaternary Science Reviews* **36**: 214–222 [DOI: 10.1016/j.quascirev.2011.04.013].

Newnham R, McGlone M, Moar N *et al*. 2013. The vegetation cover of New Zealand at the Last Glacial Maximum. *Quaternary Science Reviews* **74**: 202–214 [DOI: 10.1016/j.quascirev.2012.08.022].

Pahnke K, Sachs JP. 2006. Sea surface temperatures of southern midlatitudes 0–160 kyr B.P. *Paleoceanography* **21**: 2003–2020.

Putnam AE, Denton GH, Schaefer JM *et al*. 2010. Glacier advance in southern middle-latitudes during the Antarctic Cold reversal. *Nature Geoscience* **3**: 700–704 [DOI: 10.1038/ngeo962].

Renwick J, Thompson D. 2006. The Southern Annular Mode and New Zealand climate. *Water & Atmosphere* **14**: 24–25.

Shevenell AE, Ingalls AE, Domack EW *et al*. 2011. Holocene Southern Ocean surface temperature variability west of the Antarctic Peninsula. *Nature* **470**: 250–254 [DOI: 10.1038/nature09751].

Shulmeister J, Fink D, Augustinus PC. 2005. A cosmogenic nuclide chronology of the last glacial transition in North-West Nelson, New Zealand – new insights in southern hemisphere climate forcing during the last deglaciation. *Earth and Planetary Science Letters* **233**: 455–466 [DOI: 10.1016/j.epsl.2005.02.028].

Stuiver R. 1993. Extended ^{14}C database and revised CALIB 3.0 ^{14}C age calibration program. *Radiocarbon* **35**: 215–230.

Thompson DWJ, Solomon S, Kushner PJ *et al*. 2011. Signatures of the Antarctic ozone hole in southern hemisphere surface climate change. *Nature Geoscience* **4**: 741–749 [DOI: 10.1038/ngeo1296].

Toggweiler JR, Russell J. 2008. Ocean circulation in a warming climate. *Nature* **451**: 286–288 [DOI: 10.1038/nature06590].

Toggweiler JR, Russell JL, Carson SR. 2006. Midlatitude westerlies, atmospheric CO_2, and climate change during the ice ages. *Paleoceanography* **21**: 2005–2020 [DOI: 10.1029/2005PA001154].

Turner J, Colwell SR, Marshall GJ *et al*. 2005. Antarctic climate change during the last 50 years. *International Journal of Climatology* **25**: 279–294 [DOI: 10.1002/joc.1130].

Ummenhofer CC, England MH. 2007. Interannual extremes in New Zealand precipitation linked to modes of southern hemisphere

climate variability. *Journal of Climate* **20**: 5418–5440 [DOI: 10.1175/2007JC LI1430.1].

Vandergoes MJ, Dieffenbacher-Krall AC, Newnham RM *et al*. 2008. Cooling and changing seasonality in the Southern Alps, New Zealand during the Antarctic Cold Reversal. *Quaternary Science Reviews* **27**: 589–601 [DOI: 10.1016/j.quascirev.2007.11.015].

Vandergoes MJ, Newnham RM, Preusser F *et al*. 2005. Regional insolation forcing of late Quaternary climate change in the southern hemisphere. *Nature* **436**: 242–245 [DOI: 10.1038/nature03826].

Veblen TT, Stewart GH. 1982. On the conifer regeneration gap in New Zealand: the dynamics of *Libocedrus bidwillii* stands on South Island. *Journal of Ecology* **70**: 413–436 [DOI: 10.2307/2259912].

Wardle P. 1991. *Vegetation of New Zealand*. Cambridge University Press: Cambridge.

Williams PA. 1993. The subalpine and alpine vegetation on the central sedimentary belt of Paleozoic rocks in north-west Nelson, New Zealand. *New Zealand Journal of Botany* **31**: 65–90 [DOI: 10.1080/0028825X.1993.10419535].

Williams PW, King DNT, Zhao JX *et al*. 2005. Late Pleistocene to Holocene composite speleothem ^{18}O and ^{13}C chronologies from South Island, New Zealand – did a global Younger Dryas really exist? *Earth and Planetary Science Letters* **230**: 301–317 [DOI: 10.1016/j.epsl.2004.10.024].

Wilmshurst JM, Anderson AJ, Higham TFG *et al*. 2008. Dating the late prehistoric dispersal of Polynesians to New Zealand using the commensal Pacific rat. *Proceedings of the National Academy of Sciences* **105**: 7676–7680 [DOI: 10.1073/pnas.0801507105].

Wilmshurst JM, McGlone MS, Leathwick JR *et al*. 2007. A pre-deforestation pollen-climate calibration model for New Zealand and quantitative temperature reconstructions for the past 18 000 years BP. *Journal of Quaternary Science* **22**: 535–547 [DOI: 10.1002/jqs.1135].

Wright HE. 1967. A square-rod piston sampler for lake sediments. *Journal of Sedimentary Research* **37**: 975–976 [DOI: 10.1306/74D71807-2B21-11D7-8648000102C1865D].